BEAM DYNAMICS FOR THE NLS SUPERCONDUCTING LINAC

R. Bartolini[1,2], C. Christou[1], J.H. Han[1], I.P.S. Martin[1], J.H. Rowland[1], D. Angal-Kalinin[3], D. Dunning[3], F. Jackson[3], J. McKenzie[3], B. Militsyn[3], B.D. Muratori[3], N. Thompson[3], P.H. Williams[3]

[1]Diamond Light Source, Oxfordshire, UK, [2]John Adams Institute, University of Oxford, UK, [3]ASTeC and Cockcroft Institute, Warrington, UK.

Abstract

We present the progress with the design of the 2.25 GeV superconducting linac for the NLS project. We discuss the performance achieved, the rationale for the most recent modifications of the linac design, the relevance of microbunching instability and the analysis of the effect of various jitter sources.

INTRODUCTION

The New Light Source (NLS) project was launched in April 2008 by the UK Science and Technology Facilities Council (STFC) with the aim to develop a conceptual design for a next generation light source based on a combination of advanced conventional laser and free-electron laser sources [1]. The requirement of the science case [2] can be satisfied by a facility which has at its core a FEL driven by a 2.25 GeV energy Linac operating a high repetition rate (1 kHz and higher). The FEL operates in a seeded harmonic cascade scheme [3].

An intermediate Outline Design of the facility was produced in June 2009 [4]. The project has now reached its final stage with the CDR completion in May 2010 [2]. This paper describes the latest progress in the design and optimisation of the linac. We also discuss the operation in SASE mode and operation with the SC RF type of injector foreseen for the Phase-II of the project.

NLS LAYOUT

The NLS FELs will be driven by a single pass linac [5] using L-band superconducting cavity of TESLA type [6]. A schematic layout of the facility is shown in Figure 1. The linac has an injector consisting of an RF photocathode gun and a first accelerating structure. Initially, in Phase-I, the RF photocathode gun will be an L-band normal conducting which can be operated at 1 kHz [7]. For phase-II it is foreseen the use of a high repetition rate injector and the most promising option is a L-band superconducting RF Gun [8]. After the injector a laser heater (LH) is used to control the uncorrelated slice energy spread, a third harmonic cavity (A39) and a first accelerating module (A02) are located before the first compression (BC1) to better control the longitudinal phase space. The first compression occurs at 205 MeV. The electron beam is subsequently accelerated off-crest by two accelerating sections (A03-4) and reaches the second bunch compressors at 460 MeV. Eight accelerating modules (A05-12) bring the energy to 1.5 GeV where the last compression occurs. The beam is then accelerated on crest up to the final energy of 2.25 GeV by the remaining six modules (A13-18). A spreader distributes the beam to the three FEL lines [9].

The original NLS layout has been modified to include a merger section after the injector towards the linac, so that the commissioning of the Phase-II injector can be performed with minimal disruption on the normal operation of the machine.

With respect to the initial design [4-5], the operating gradient, initially set to 20 MV/m, has been reduced to 15 MV/m considering the most cost effective solution for both capital and operating cost of the facility. This has required the introduction of four more accelerating sections bringing the total number to eighteen.

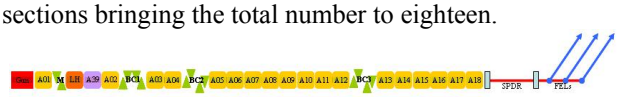

Figure 1: Schematic layout of the NLS FEL showing the location of gun, merger section (M), laser heater (LH), accelerating section (A01-A18), third harmonic cavity (A39), bunch compressors (BC1-3) and spreader section to the FELs.

NLS BEAM DYNAMICS

The linac working point has been optimized with the aim of generating a bunch with low slice normalized emittance (< 1 μm), low slice relative energy spread (< 10^{-4}) and sufficient peak current (> 1 kA). Various operating charges were considered. A reasonable management of the collective instabilities proved possible for charges below 200 pC.

The operation in a seeded scheme adds further constraints to the target beam quality. In fact, the requirement of a high degree of temporal coherence implies that the slice beam parameters along the seed laser pulse length (20 fs FWHM) has to be as constant as possible. If significant variations in slice properties exist, the high gain FEL process will amplify them, generating again a spiky profile with poor temporal coherence. Furthermore, timing jitter errors between the electron bunch and the seed laser pulse have been estimated to be 16 fs rms as shown in the section on Linac Jitters Studies. To accommodate these errors, constant slice parameters have to be provided over a length of about 100 fs.

The linear optics of the linac, reported in Figure 2, is characterized by a focussing system built along the RF accelerating modules with quadrupoles in-between each module. The merger section from the injector to the linac is a simple dogleg. Triplets of quadrupoles are used on either side of the bunch compressors to match to the linac

channel and to minimize the horizontal beta function at the fourth dipole, a condition that minimizes the effect of CSR at the compressor.

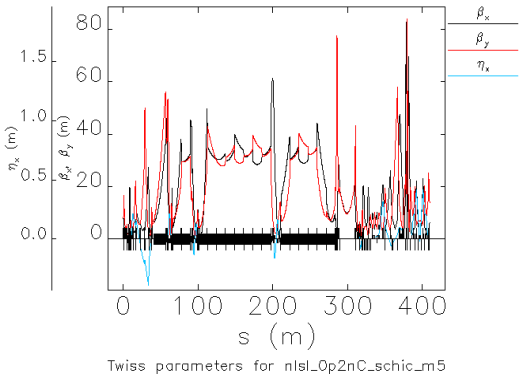

Figure 2: Optics functions of the linac from the merger section to the spreader.

The beam dynamics in the merger is considerably simplified if the electron beam coming from the injector has no energy chirp. In this way chromatic effects due to the large dispersion in the merger are greatly reduced. The energy chirp in the longitudinal phase space necessary for the compression in BC1 is imparted before BC1 by the second accelerating module (A02). A third harmonic cavity (A39) was introduced to linearize the longitudinal phase space before the compression. The optimal decelerating voltage was found to be 35 MV, corresponding to a gradient of 13.1 MV/m and a phase of -96.5 degrees for the 3.9 GHz module.

Concerning the compression, we have adopted a strategy whereby the first bunch compressor BC1, which acts at a relatively low energy of 205 MeV, produces only a moderate compression which is nevertheless sufficient to redistribute the task of the compression in a more relaxed way within the last two compressors. With the present design the compression ratio of the three bunch compressors is 2.0, 4.0 and 10.4 respectively. The bunch length from the injector is 15 ps full width half maximum (FWHM) and is reduced to 180 fs FWHM at the beginning of the undulators. Each compressor consists of four dipoles separated by drift spaces whose length has been varied in order to minimize the effect of the CSR. During the course of the optimisation we found that the most effective control of CSR effects is obtained using C-type compressor in BC1 while we used S-type compressors in BC2 and BC3 [5]. The longitudinal phase space evolution of the beam along the linac is reported in Figure 3. This optimisation guarantees that a high electron beam peak current (> 1 kA) and slice emittance and relative energy spread of the order of 1 μm and 10^{-4} respectively, as shown in Figure 4.

The final validation of the optimisation was done time-dependent SASE simulations with GENESIS [10]. Assuming the undulator parameters of the radiator in FEL-3 described in [3], the results reported in Figure 5 show that these beam parameters generate a FEL gain length sufficient to reach saturation within 40 m at 1 keV.

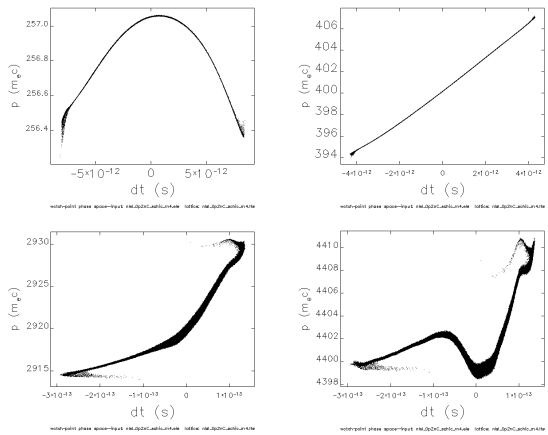

Figure 3: Longitudinal phase space at different locations in the linac: top left - after the 1st accelerating module; top right - after BC1; bottom left - after BC3; bottom right - at the end of the spreader

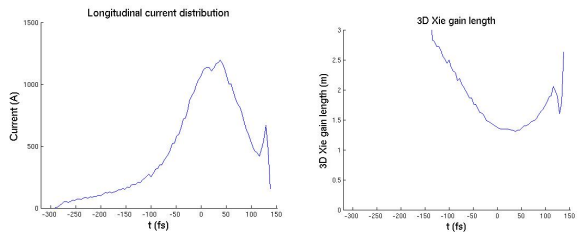

Figure 4: Longitudinal current profile (left) and corresponding 3D Xie gain length (right) at the end of the spreader. The right graph shows a flat region of about 100 fs with a 3D Xie gain length variation within 10%.

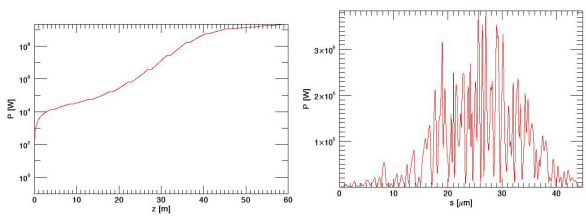

Figure 5: SASE power along the undulator and corresponding pulse profile at 40 m

As a fall-back option we also investigated the possibility of generating short radiation pulses in SASE mode with FWHM of about 20 fs. This can be achieved by reducing the operating charge to 50 pC and shortening the electron bunch length by compressing more aggressively the electron bunch. It was possible to show that the present linac layout SASE saturation at GW power level can be reached less than 40 m. The FEL pulse length can be controlled within 5 to 30 fs FWHM and the corresponding time bandwidth product is within 5 to 30.

LINAC JITTERS STUDIES

The analysis of the effect of various jitter sources on the operation of the linac and the injector has been carried out numerically in order to assess the final electron beam qualities. The jitter sources considered in our study are summarised in Tab. 1.

Tab. 1: Jitter amplitudes (rms) used in the initial simulations.

RF gun phase	0.1 deg
RF gun voltage	10^{-3}
Gun solenoid field rel.	10^{-4}
Main RF cavity phase	0.01 deg
Main RF cavity voltage	10^{-4}
BCs power supplies	$5{\cdot}10^{-5}$

The beam dynamics has been analysed with full start-to-end simulations from the RF photocathode gun with ASTRA[11] and through the linac with elegant[12]. The rms of the Gaussian random distribution of the quantities subject to jitters are defined on the basis of the operational experience at FLASH or modest improvement of these. In order to reduce the effect of the jitter on the arrival time it was assumed that each RF cavity in each module can be fed independently. In this way the effect of the random jitter adds in quadrature and the detrimental effect of correlated errors can be avoided. The results of the jitter studies are summarised in Tab. 2 and in Figures 6-7, where the effect of the jitters sources on the FEL performance is also reported. The average power of the FEL in the seeded scheme is 1.4 GW at 23 m in the undulator, with a variation of less than 30% rms.

Tab. 6: Arrival time jitter (rms) with RF split in ACC01 and reduced jitter in bunch compressor power supplies.

RF gun (P and V)	9 fs
Injector (RG Gun + ACC01)	12 fs
Linac P + V + B combined	12 fs
P + V + B + I combined	16 fs

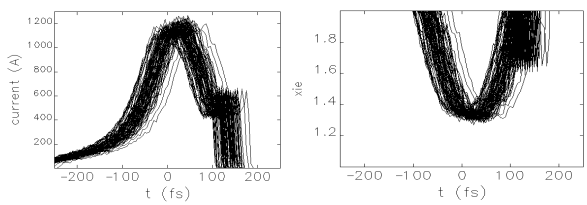

Figure 6: Longitudinal profile of 100 jitter electron bunches (left) and corresponding 3D Xie gain length.

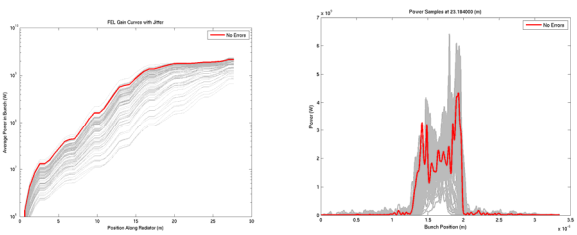

Figure 7: power as a function of the undulator length for 100 random seed (left), corresponding pulse profile (right) for the seeded scheme of [3]

LINAC WITH PHASE II INJECTOR

In view of the operation at high repetition rate the NLS Linac and FELs will operate in a second stage with a high repetition rate superconducting RF gun [8]. Despite being in its early stages, the optimization of the beam dynamics has produced an electron bunch with interesting quality. In particular, the transverse slice emittance is comparable with the one achieved in the stage-I normal conducting L-band gun, however at the expenses of a significantly longer bunch length. The linac layout described so far is capable of compressing also this longer bunch with good control of the collective effects as shown in Figures 8-9.

SASE operation with such an electron bunch show that saturation at GW power level can be reached in 42 m. This confirms that the NLS FELs can be operated successfully with a linac driven by a SC RF gun.

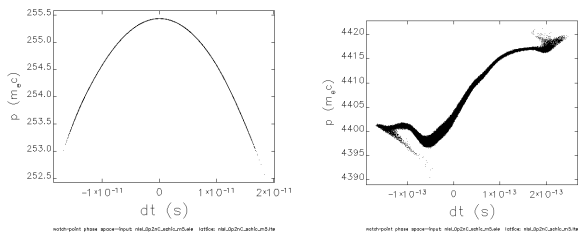

Figure 8: Longitudinal phase space at different location in the linac: left - after the first accelerating module A01; right at the end of the spreader

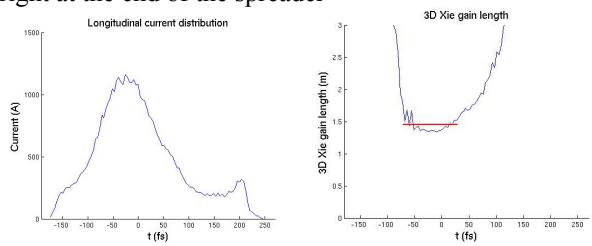

Figure 9: Longitudinal current distribution (right) and 3D Xie gain length (right) at the end of the spreader.

CONCLUSIONS

We have presented a design of the linac which can deliver an electron beam of sufficiently good quality to drive a FEL at 1 keV using a seeded harmonic cascade approach. The results are supported by numerical simulations including extensive jitter studies. The design is compatible with the operation with a SC RF injector.

REFERENCES

[1] R.P. Walker et al., these proceedings
[2] See www.newlightsource.org NLS Project Conceptual Design Report, (2010).
[3] D. Dunning et al., these proceedings.
[4] NLS Science Case and Outline Facility Design in [2].
[5] R Bartolini et al., pg. 480, FEL09 proceedings (2009).
[6] D. Proch, TESLA Note 1994-13, (1994).
[7] J.H. Han et al, pg. 340, FEL09 proceedings (2009).
[8] J.W. McKenzie et al., these proceedings.
[9] D. Angal-Kalinin et al, these proceedings
[10] S. Reiche, Nucl. Inst. And Meth. **A429**, 243, (1999)
[11] K. Floettmann, A Space Charge Tracking Algorithm (ASTRA), http://www.desy.de/~mpyflo.
[12] M. Borland, APS LS-287, (2000).